SPIXIANA	39	1	39–60	München, September 2016	ISSN 0341–8391

Detailed description of a giant polychelidan eryoneicus-type larva with modern imaging techniques

(Eucrustacea, Decapoda, Polychelida)

Stefan M. Eiler, Carolin Haug & Joachim T. Haug

Eiler, S. M., Haug, C. & Haug, J. T. 2016. Detailed description of a giant polychelidan eryoneicus-type larva with modern imaging techniques (Eucrustacea, Decapoda, Polychelida). Spixiana 39 (1): 39–60.

Polychelida occupies an important phylogenetic position within Decapoda. All modern representatives of this monophyletic group inhabit the deep sea and show a mixture of traits known from different other decapod groups. For example, they share some derived characters with Eureptantia and retain ancestral ones, which they share with, e. g. Caridea. In their specific systematic position, somewhere between Caridea and Eureptantia, they can be seen as an evolutionary link between these groups. More precisely, their morphotype combines aspects of the 'shrimp' morphotype and of the 'lobster' morphotype. Just to name some examples, representatives of Polychelida have 1) a triangular telson, which is an ancestral trait they share with the 'shrimp' morphotype, whereas the 'lobster' morphotype has a rectangular telson, and 2) their dorso-ventrally compressed pleon is a typical trait of Eureptantia ('lobster' morphotype), while representatives of Caridea still have a laterally compressed pleon ('shrimp' morphotype). Additionally, modern polychelids show peculiarities of their own evolutionary lineage. Most strikingly, besides the fact that all modern forms are blind, is that the benthic modern adulti develop from highly specialized pelagic larvae, which can reach a size of several centimeters and thus represent giant larvae. We present a detailed documentation of a modern giant eryoneicus larva taking advantage of composite autofluorescence imaging. This includes several outer structures, such as the thoracopods and pleopods, but also inner structures, such as their gizzard and its masticatory organs. Additionally, we provide the first high-resolution 3D photographs of such a larva to show its morphological structures in situ with correct topology.

Stefan M. Eiler (corresponding author), Department of Biology II and GeoBio-Center, LMU Munich, Großhaderner Str. 2, 82152 Planegg-Martinsried, Germany; e-mail: stefan-eiler@gmx.de

Carolin Haug & Joachim T. Haug, Department of Biology II and GeoBio-Center, LMU Munich, Großhaderner Str. 2, 82152 Planegg-Martinsried, Germany

Introduction

Polychelida is a comparably small monophyletic group of lobster-like decapod crustaceans, comprising only about 37 extant species worldwide (Ahyong 2012). Many details of the group are still very little-known, as the modern polychelid lobsters (Polychelidae) are exclusive deep-sea inhabitants (Galil 2000, Ahyong 2009) and there are not too many collected specimens examined in detail so far.

The most obvious character of polychelids is that adult polychelids always bear true chelae on thoracopods 4–7 (pereiopods 1–4; Scholtz & Richter 1995). Females additionally bear a chela on the thoracopod 8 (pereiopod 5). In some species both sexes bear a true chela there (Bernard 1953, Williamson 1983).

Polychelida is an ingroup of Reptantia (Scholtz & Richter 1995), the group comprising lobsters, crabs and ghost shrimps. Hence, polychelids possess many lobster-type characters, such as a dorso-ventrally compressed body form and a straight pleon (Scholtz & Richter 1995). Yet, Polychelida has been resolved as the sister group to all remaining reptantians (Eureptantia; Scholtz & Richter 1995), as polychelids retain some plesiomorphic features, which they share with shrimps but which are absent in other reptantians.

As modern polychelids are inhabitants of the deep sea, also specialized adaptations to this specific habitat have evolved. As the probably most obvious one, all modern polychelids are blind. Their compound eyes have become reduced, in most cases the eye stalks are retained (Galil 2000, Ahyong 2009).

Another highly specialized adaptation, which is not necessarily coupled to their deep-sea habitat, is their post-embryonic ontogeny: the benthic, blind and deep-sea inhabiting adults (Galil 2000, Ahyong 2009) develop from highly specialized pelagic larvae. Those larvae can grow up to several centimeters and are therefore representing giant larvae. Giant larvae have evolved in different crustacean lineages such as mantis shrimps (Gamô 1979) and achelate lobsters (Johnson 1951) and represent a fascinating ecological adaptation to quite long life in the planktic regime.

Due to their phylogenetic position Polychelida has the potential to resolve important details of the evolution of Reptantia. On the other hand, modern polychelids are highly derived due to their numerous adaptations to their deep-sea habitat and their giant larvae. Hence a detailed understanding of these adaptations fulfils three functions: 1) it identifies specializations of the lineage, which are not part of the ground pattern of Reptantia, hence makes a contribution to the evolution of lobsters and 2) can inform about adaptations to the deep-sea habitat and 3) can inform about the evolution of giant larvae as a specialized ecological adaptation.

Unfortunately, our knowledge about the larvae is even more limited than our knowledge about the adults. The material examined by now has mostly been centered on adult specimens. The few examined polychelidan larvae have usually been documented by drawings (Bernard 1953, Galil 2000, Ahyong 2009) and/or by overview photographs. Notable exceptions for good quality photographs of eryoneicus zoea larvae are Torres et al. (2014), for detailed photography of an eryoneicus megalopa see Hernández et al. (2007) or Martin (2014a).

The eryoneicus larvae show very peculiar and highly specialized morphology. They have long been thought to be adults of a monophyletic group, so they were named *Eryoneicus* as a genus name. Yet, now *"Eryoneicus"* is an invalid taxonomic name as it only represents a larval morphotype of Polychelidae (Bernard 1953, see also discussion in HaugJT et al. 2013a).

Despite this "new" awareness the larvae still cannot get associated with the respective adults of the different species, except for *Eryoneicus puritanii*, which could get assigned with *Polycheles typhlops* as Guerao & Abelló (1996) hatched eggs from a gravid *P. typhlops* female in captivity. Although these larvae showed morphological differences to those hatched under natural conditions they could get assigned with each other. This also got proven by Torres et al. (2014) with DNA analyses.

To understand the evolution of highly specialized larval forms fossils can contribute less specialized evolutionary intermediates. HaugJT et al. (2015) found that the polychelid larvae evolved in a stepwise manner, as indicated by a 90 million year old (Ma) fossil representative. Additionally, we need to improve our knowledge of morphological details of the modern forms.

Here we provide the first intensive documentation of an eryoneicus larva with up-to-date imaging methods including high-resolution 3D photography and composite autofluorescence. We present numerous details of the larva's outer structures such as details of shield, pleon and especially the appendages, but also some inner structures such as the gizzard and its masticatory organs. With this we provide new insights into the morphology of an eryoneicus larva.

Material and methods

Material

Specimen used in this study came from the Muséum National d'Histoire Naturelle in Paris; yet, originally the specimen was part of the Zoological State Collection in Munich, according to the label. The specimen was labelled as *"Eryoneicus" atlanticus*. Yet, the name *"Eryoneicus"* is no longer valid (Bernard 1953, see also HaugJT et al. 2013a) as it only represents a larval morphotype of polychelid lobsters. The collection number of the studied specimen is MNHN-IU-2009-3168.

Documentation

Two principle types of documentation were applied:

1) At first the eryoneicus larva was documented with a Canon EOS Rebel T3i digital camera and a Canon MP-E 65 mm lens, which was mounted on a swivel arm to have the ability to rotate the camera around the larva. To get the ideal focus we used the adjustable microscope on which we placed the material. To optimise illumination we used a Canon Macro Twin Lite MT-24EX flash. The larva was immersed in 70 % ethanol on a black surface; a large microscopic cover slip was placed on top of the specimen, so it could not move during the

photographic process. To reduce the reflections caused by the flash we used two polarisers in front of the two flash lights and one perpendicular polariser in front of the lens of the camera (HaugC et al. 2011, Kerp & Bomfleur 2011). Images were taken from many different angles within nearly 180 degrees around the larva. We photographed it from ventral, dorsal and both lateral sides. Afterwards images were edited in Adobe Photoshop CS6; two images slightly differing in angle of view were used to produce a stereo anaglyph of them.

After documenting the larva as a whole the specimen was dissected in a step-wise manner. The pleon was removed from the thorax. Then the pleopods 2 to 5, the thoracopods 4 to 8 and the mouthparts (maxillipeds 1 to 3, maxilla 1 and 2 and mandibles) were dissected off. The remaining parts of head and thorax were removed from the shield; only antennulae and antennae remained attached to it.

The shield was then also photographed from dorsal, ventral and both lateral sides with the camera mounted on a swivel arm as described above. Additionally, it was photographed from anterior and posterior without the swivel arm by using the Canon EF-S 18–55 mm lens and a 31 mm extension tube; to overcome limitations in the depth of field the focus was gradually changed and thus a stack of images was recorded. The resulting stack was fused to a completely sharp image by using the computer program CombineZM. After documenting the shield the antennulae and antennae were removed from it.

2) Remaining parts were documented on a Keyence BZ-9000 fluorescence microscope by composite autofluorescence imaging (HaugJT et al. 2008, 2011a, Kerp & Bomfleur 2011, HaugC et al. 2012). This was facilitated by the autofluorescence capacities of the cuticle (HaugC et al. 2011, HaugJT et al. 2011a, Kutschera et al. 2012, Rötzer & HaugJT 2015). Objectives used were 2×, 4× and 10× resulting in 20×, 40× and 100× magnification. Wavelength used was 520 nm.

The first pleopods and the uropods were dissected off the pleon after it had been documented in one piece. Afterwards also the pleopods and uropods were documented separately. Besides the pleon and all appendages, we also dissected and documented the gizzard still connected to the labrum and the paragnaths. Later also the individual gizzard teeth and the reusen-apparatus were dissected off and then documented.

Also here images were recorded as stacks and then fused with CombineZM or CombineZP. Furthermore, several image details had to be documented because of their size of the structures and then stitched to a single panorama image using Microsoft Image Composite Editor or the photomerge function of Adobe Photoshop CS3.

In some images documentation was difficult because of their wide range of brightness. So, at first, they were recorded in "normal" illumination, so the details in the dark areas could hardly be seen but structural detail in the bright areas were visible. Therefore, these images were also recorded with over-exposure, afterwards, which highlighted the details in the dark areas but left the bright areas without information. In Adobe Photoshop CS3 or CS5 the overexposed images were placed on top of the normally exposed images as separate layers. Then the overexposed (white) areas were marked with the magic wand tool, assigned a feather and cut out; so the structural details of the underlying layer became visible but the highlighted details of the top layer were still retained. In this way we received combined images with full information (HaugC et al. 2013).

The images were edited with Adobe Photoshop CS3 or CS5 subsequently; by using the lasso-tool all the dirt and artifacts were removed from the images and the filter 'mask unsharp' was applied. To perceive every little detail the brightness was adjusted in 'levels'.

Description

To provide an extensive description, a descriptive matrix was created (HaugJT et al. 2012). This matrix is available as electronic supplement.

Results

The examined larva is a small arthropod larva with a strongly arched shield. Its total size is about 50 mm. The body is differentiated into cephalothorax, pleon and a non-somitic telson. The body consists of 20 segments divided into an ocular segment plus 19 appendage-bearing (post-ocular) segments (Fig. 1).

The ocular segment is incorporated into the cephalothorax, the dorsal area contributes to the shield (cephalothoracic shield, carapace). The post-ocular segments 1–13 are also incorporated into the cephalothorax, whereby the dorsal area contributes to the shield. The following post-ocular segments 14–19 are separate pleon segments, which are each dorsally forming a tergite (Fig. 1).

In dorsal view the shield shape is more or less oval and about as long as maximum width. The anterior rim of the shield is drawn out into a rostrum flanked by 2 anterior directed spines. The rostrum is trapezoid-shaped. The ventral rim (Fig. 2) and the posterior rim (Fig. 3) of the shield have numerous setae on the inside. On the dorsal side of the shield the anterior third is separated from the posterior two-thirds by a cervical groove. Dorsally in the anterior third, 4 spines are present in an anterior-posterior row. In the posterior two-thirds, 2 rows of spines are present in anterior-posterior direction. Furthermore, it is armed with 2 rows of spines on each lateral side and 1 row of larger spines on each ventral side. The upper lateral rows consist of 6 spines each; the most anterior spine of each row is right at the posterior rim of the cervical groove. The lower lateral rows consist of 18 spines which are directed anteriorly. The most anterior spines are flanking the rostrum

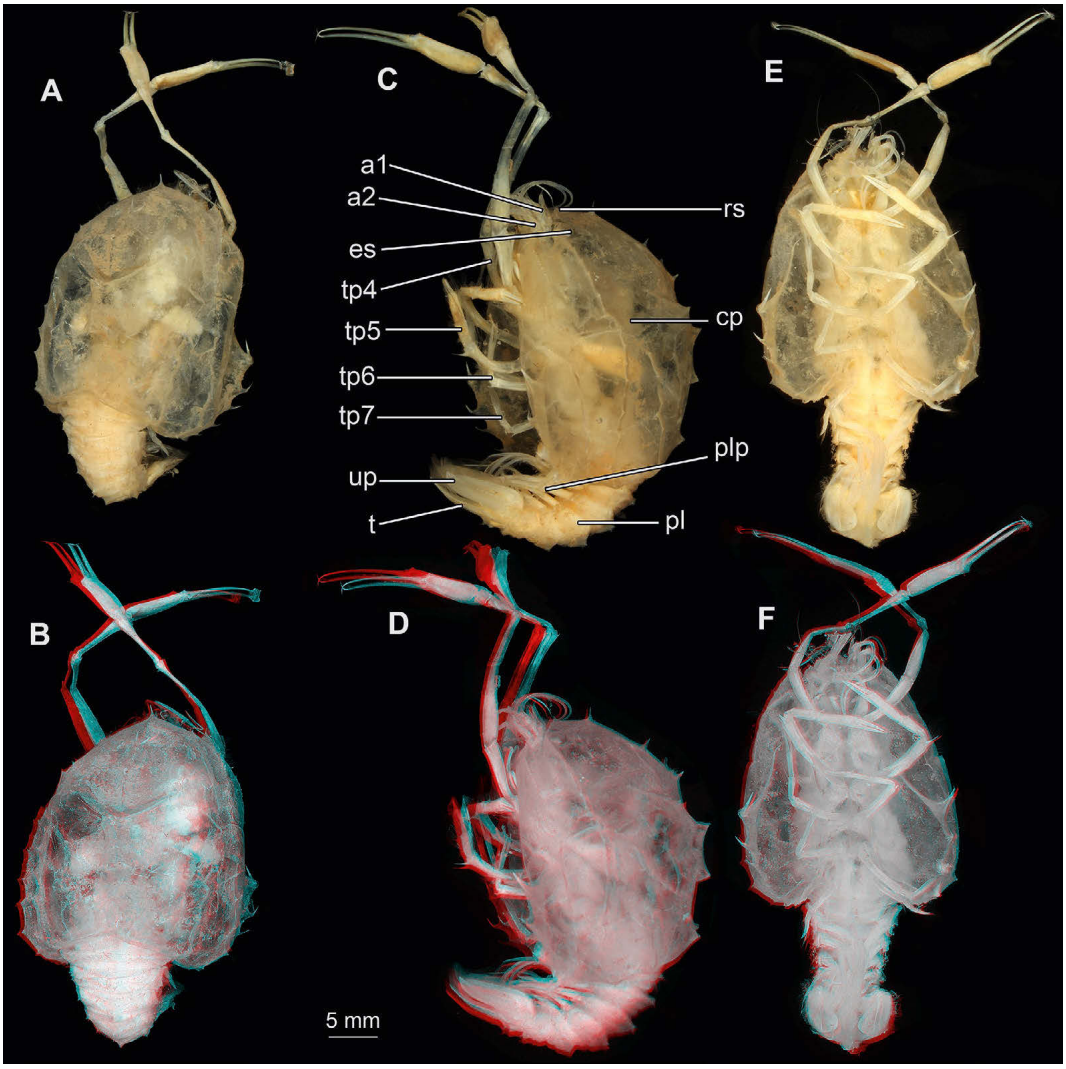

Fig. 1. Overview of examined eryoneicus larva. **A.** Dorsal view; **B.** dorsal view, stereo anaglyph; **C.** lateral view (left); **D.** lateral view (left), stereo anaglyph; **E.** ventral view; **F.** ventral view, stereo anaglyph. Abbreviations: **a1**, antennula; **a2**, antenna; **cp**, carapace (shield); **es**, eye stalks; **pl**, pleon; **plp**, pleopods; **rs**, rostrum; **t**, telson; **tp**, thoracopod; **up**, uropod.

as mentioned above. The ventral rows consist of 4 spines each, which are directed anteriorly and become smaller from anterior to posterior (Fig. 2).

The anterior-posterior dimension of the post-ocular segment 14 (pleomere 1; Fig. 4) is about 15 % of the shield length. Its total width is about 45 % of the shield width. The axial region equals to the total width of the segment. The tergo-pleura are apparently transformed into hook-like structures directed laterally (described as knob-like structures by Scholtz & Richter 1995; Fig. 4). The tergo-pleura are about one fifth of the axial region, on each side. On the distal rim of the axial region there is a row of about 120 setae. Furthermore, post-ocular segment 14 is armed with 2 spines at the base of the hook-like structures on each side and 1 spine dorsally in the middle.

The anterior-posterior dimension of the post-ocular segment 15 (pleomere 2; Fig. 4) is about 10 % of the shield length. Its total width is slightly smaller than that of the preceding segment. The axial region equals to the total width of the segment. The tergo-pleura are straight, directed ventrally and about one

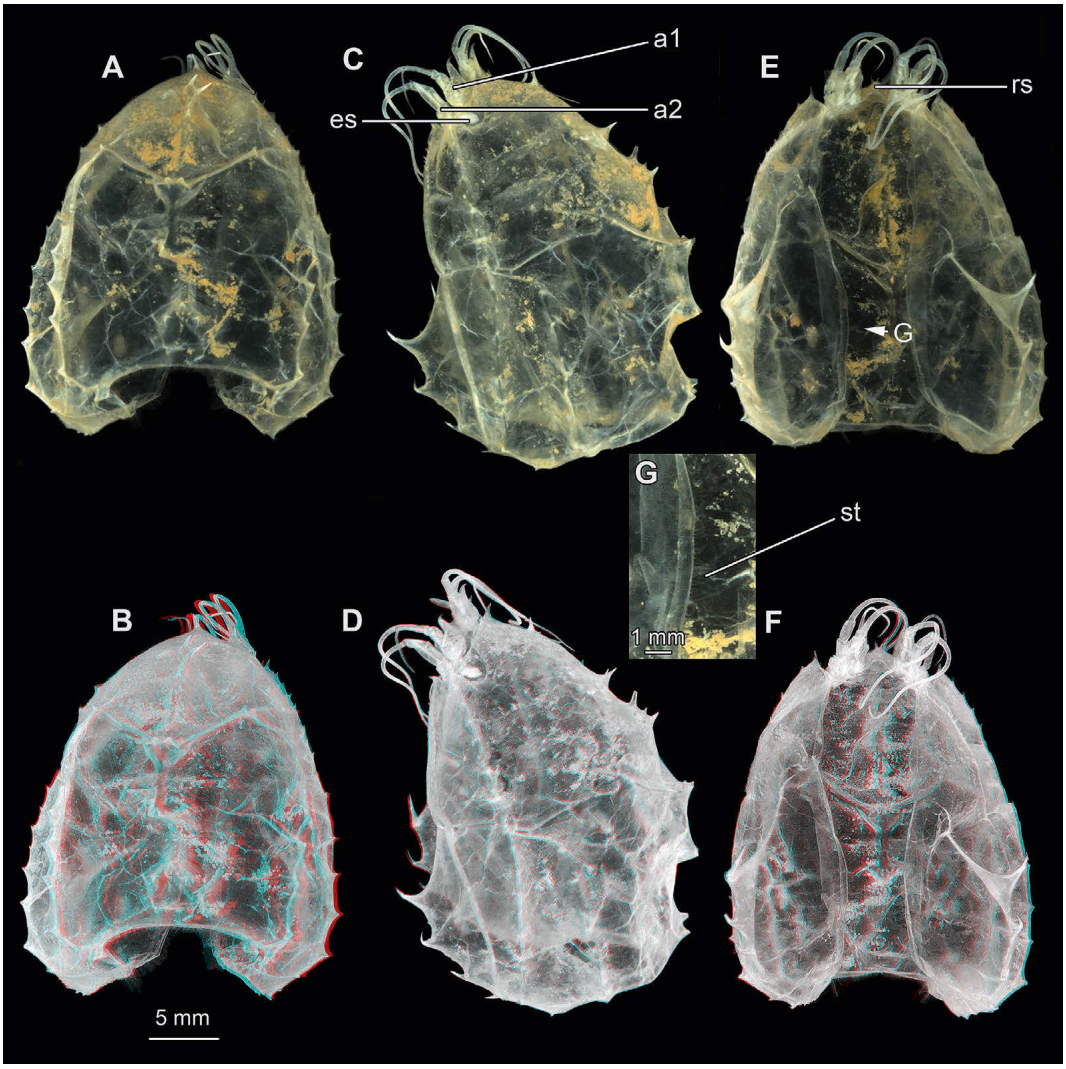

Fig. 2. Overview of isolated shield. **A.** Dorsal view; **B.** dorsal view, stereo anaglyph; **C.** lateral view (left); **D.** lateral view (left), stereo anaglyph; **E.** ventral view; **F.** ventral view, stereo anaglyph; **G.** detailed view of setae on ventral rim of shield. Abbreviations: **a1**, antennula; **a2**, antenna; **es**, eye stalks; **rs**, rostrum; **st**, setae.

half of the axial region, on each side. On the distal rim of the axial region a row of about 100 setae can be seen. Furthermore, post-ocular segment 15 is armed with 1 spine on the distal end of each lateral side and 1 spine dorsally in the middle.

The anterior-posterior dimension of the post-ocular segment 16 (pleomere 3; Fig. 4) is about 10 % of the shield length. Its total width is slightly smaller than that of the preceding segment. The axial region equals to the total width of the segment. The tergopleura are straight, directed ventrally and they are about one half of the axial region, on each side. On the distal rim of the axial region is a row of about 80 setae. Moreover, post-ocular segment 16 is armed with 2 spines on the distal end of each lateral side and 1 spine dorsally in the middle.

The anterior-posterior dimension of the post-ocular segment 17 (pleomere 4; Fig. 4) is about 10 % of the shield length. Its total width is slightly smaller than that of the preceding segment. The axial region equals to the total width of the segment. The tergopleura are straight, directed ventrally and they are about one half of the axial region, on each side. On the distal rim of the axial region a row of about 70

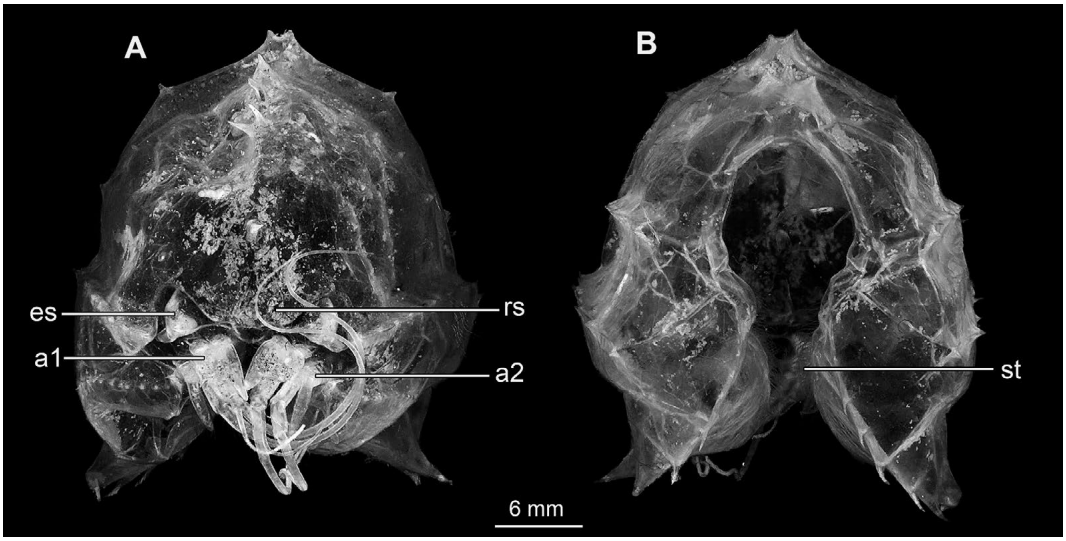

Fig. 3. Isolated shield in anterior (**A**) and posterior (**B**) view. Abbreviations: **a1**, antennula; **a2**, antenna; **es**, eye stalks; **rs**, rostrum; **st**, setae.

setae can be seen. Besides, post-ocular segment 17 is armed with 2 spines on the distal end of each lateral side and 1 spine dorsally in the middle.

The anterior-posterior dimension of the post-ocular segment 18 (pleomere 5; Fig. 4) is about 10 % of the shield length. Its total width is slightly smaller than that of the preceding segment. The axial region equals to the total width of the segment. The tergopleura are directed ventrally with a slightly laterally curved tip and they are about 65 % of the axial region, on each side. On the distal rim of the axial region there is a row of about 60 setae. Post-ocular segment 18 is armed with 2 spines on the distal end of each lateral side and 1 spine dorsally in the middle.

The anterior-posterior dimension of the post-ocular segment 19 (pleomere 6; Fig. 4) is about 10 % of the shield length. Its total width is slightly smaller than that of the preceding segment. The axial region equals to the total width of the segment. The tergopleura are directed ventrally with a strongly laterally curved spiny tip and they are about 60 % of the axial region, on each side. On the distal rim of the axial region a row of about 40 setae is apparent.

The shape of the telson (Fig. 4) in dorsal view can be divided into two parts. The two parts can be described as a rectangular proximal region and an elongate triangular distal region with a pointed tip. In lateral view the telson is scimitar-shaped. In the triangular region 2 dorsal rows of about 16 spines can be seen. On each lateral rim the telson is featuring about 9 spines. Setae can be seen around the distal end of the rectangular part and the entire triangular part of the telson. There are about 110 setae on each lateral rim of the telson, which have a uniform size at the triangular and the rectangular part each.

The lateral eyes are reduced, therefore only eye stalks are retained (Fig. 3).

The hypostome-labrum complex has a u-shaped labrum (ventral view), which is anteriorly surrounded by the hypostome (cf. Fig. 13).

Appendage 1 (antennula; Fig. 5) is differentiated into a peduncle and 2 flagella. It is about half the size of the shield. The peduncle consists of 3 elements: Peduncle element 1 is rectangular-shaped and nearly as wide as long. It has a small protrusion on the outer lateral rim and an elongate protrusion on the inner lateral rim at the distal end of the element. The inner lateral protrusion is about 3 times as long as the outer lateral protrusion and with about 40 setae on the outer lateral rim. The peduncle element 2 is about two-thirds of peduncle element 1. It is tube-shaped and nearly as wide as long. The peduncle element 3 is about two-thirds of peduncle element 2, tube-shaped and as wide as long. The 2 flagella emanate from the third peduncle element. While flagellum 1 consists of 59 flagellomeres with 3–4 setae at every second flagellomere, flagellum 2 consists of 19 flagellomeres with 4 setae at the tip of the terminal flagellomere.

Appendage 2 (antenna; Fig. 5) is differentiated into peduncle, exopod and endopod, which is distally bearing a flagellum. It is about as long as the preceding appendage. The peduncle consists of 2 elements: Peduncle element 1 (coxa) has a long protrusion

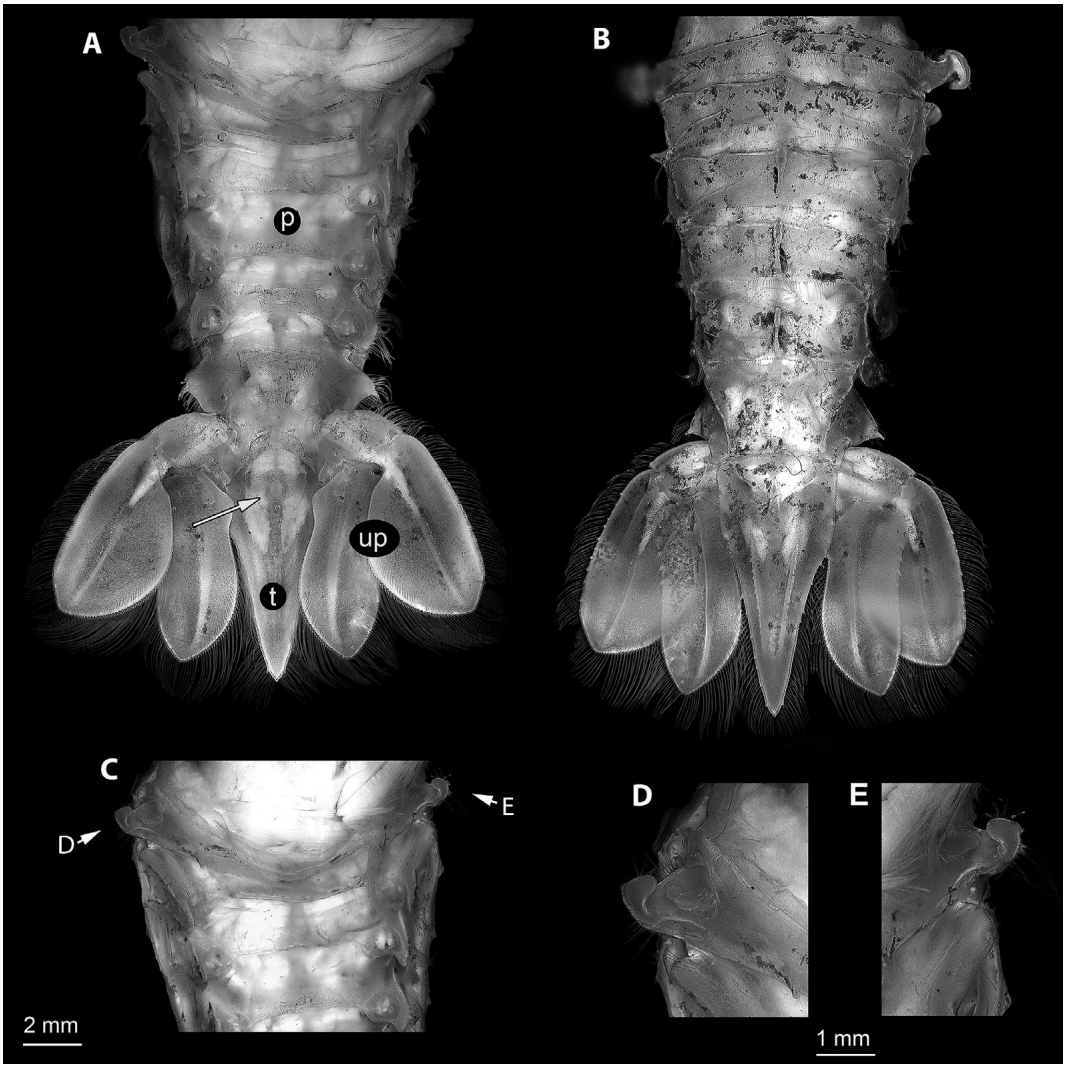

Fig. 4. Pleon overview still with uropods and telson. **A.** Pleon ventral, with anus on telson (arrow); **B.** pleon dorsal; **C.** pleon ventral, focus on hook-like structures on the first pleon segment; **D–E.** detailed view of the knob-like structures. Abbreviations: **p**, pleon; **t**, telson; **up**, uropods.

with an excretory opening. The peduncle element 2 (basipod) is tube-shaped and twice as wide as long. The endopod of appendage 2 consists of 3 elements and 1 flagellum: Endopod element 1 is tube-shaped and twice as long as wide. Endopod element 2 is tube-shaped. It is slightly shorter than endopod element 1, twice as long as wide and with about 10 setae. Endopod element 3 is tube-shaped and about one quarter of the size of endopod element 1 and 2. The exopod is paddle-shaped with about 40 setae. The flagellum consists of 54 flagellomeres with 3–4 setae at about every second flagellomere.

Appendage 3 (mandible; Fig. 6) is differentiated into a coxa with an endite and a mandibular palp. It is about one quarter of the size of the preceding appendage. The coxa is elongated and ending in an endite with 17 teeth at the left mandible and 11 teeth at the right mandible. Between molar and incisor part no clear distinction is visible (see also Torres et al. 2014; Fig. 7). The mandibular palp consists of 3 elements and is covered with numerous setae: Mandibular palp element 1 is triangular from anterior and posterior view. The mandibular palp element 2 is more or less tube-shaped and slightly curved.

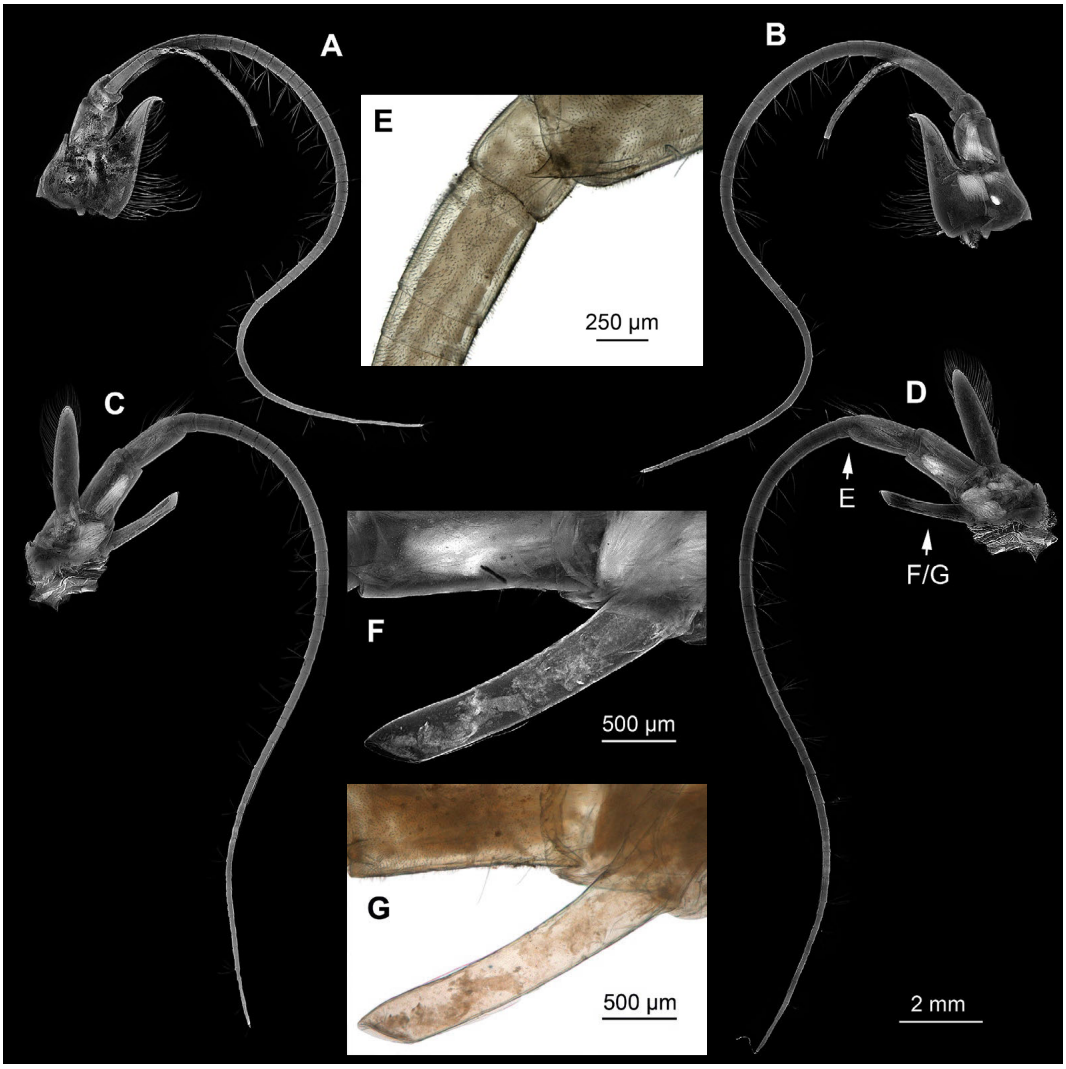

Fig. 5. Fluorescence microscopic overview (**A–D**) and detail (**F**) of the right antennula and antenna and transmitted white-light microscopic details (**E/G**) of the right antenna. **A.** Antennula, anterior; **B.** antennula, posterior; **C.** antenna, anterior; **D.** antenna, posterior; **E.** detailed view of the proximal region of the flagella of the antenna; **F–G.** detailed view of the coxal appendage with excretory opening of the antenna on distal end.

It is twice as long as the mandibular palp element 1 and about 3 times as long as wide. The mandibular palp element 3 is paddle-shaped with a rounded tip. It is as long as mandibular palp element 2 and about 3 times as long as maximum width. A sternal protrusion of the mandibular segment can be seen (paragnaths; Fig. 13). It is u-shaped with 2 lateral elongate hook-like protrusions at the proximal end. It is about as large as the hypostome-labrum complex and about twice as wide as long.

Appendage 4 (maxillula; Fig. 6) is differentiated into coxa with a coxal endite and basipod with a basipodal endite. It is about half the size of the preceding appendage. The coxal endite is thin paddle-shaped, curved and with numerous setae. The basipodal endite is thin paddle-shaped, curved, with numerous setae and 3 setae-like spines at the tip (Fig. 7). It is slightly larger and about twice as wide as the coxal endite.

Appendage 5 (maxilla; Fig. 6) is differentiated into a proximal part, a distal part and an exopod. It is about twice as large as the preceding appendage. The

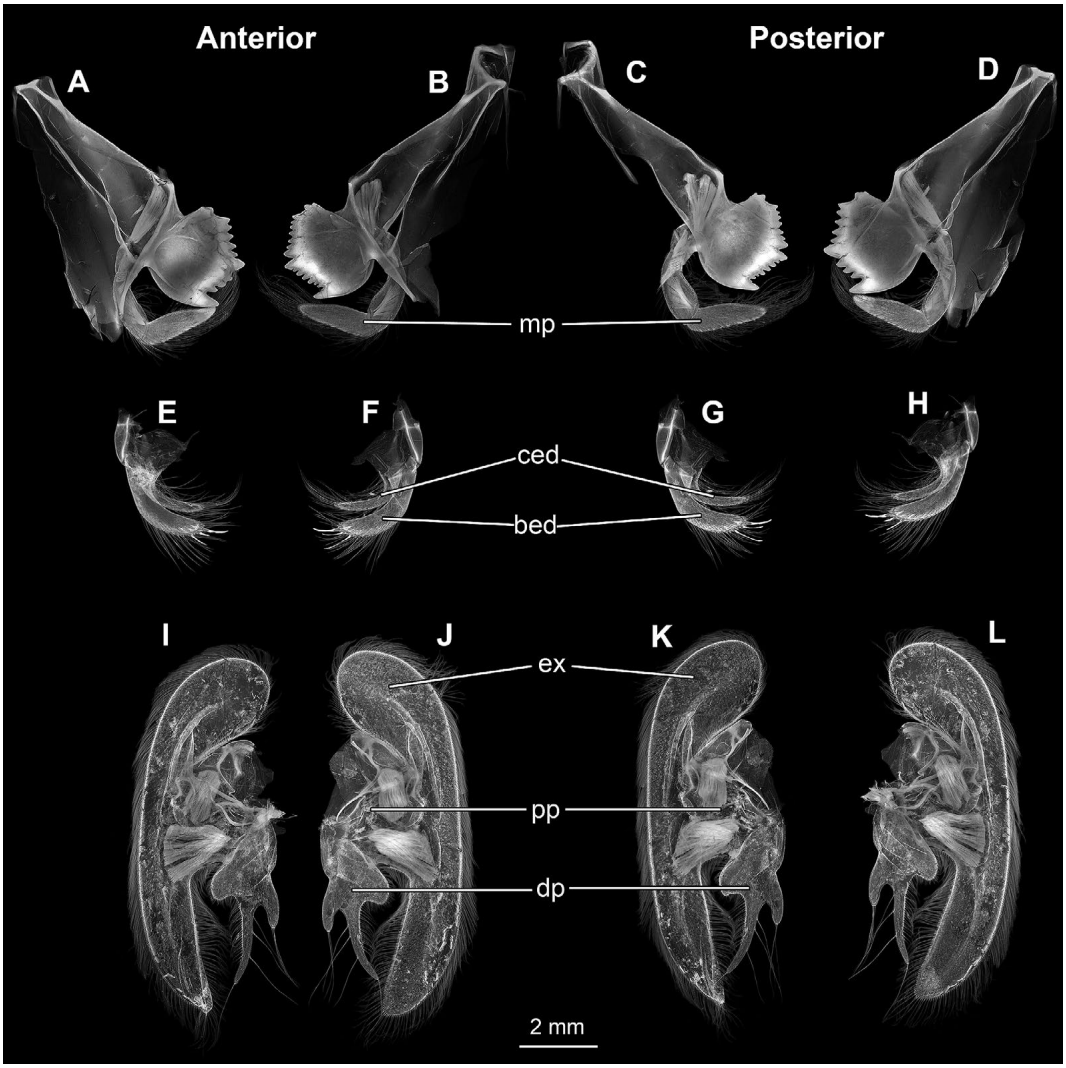

Fig. 6. Overview of mouthparts. **A.** Right mandible, anterior; **B.** left mandible, anterior; **C.** left mandible, posterior; **D.** right mandible, posterior; **E.** right maxillula, anterior; **F.** left maxillula, anterior; **G.** left maxillula, posterior; **H.** right maxillula, posterior; **I.** right maxilla, anterior; **J.** left maxilla, anterior; **K.** left maxilla, posterior; **L.** right maxilla, posterior. Abbreviations: **bed**, basipodal endite; **ced**, coxal endite; **dp**, distal part; **ex**, exopod; **mp**, mandibular palp; **pp**, proximal part.

proximal part is probably corresponding to coxa and basipod, but it is difficult to find a clear distinction. The distal part has 3 different sized lobes: The inner lobe has 2 uniform setae and is about twice as long as maximum width. The middle lobe has about 3 setae on the inner rim, which are of the same size as those on the inner lobe, and 1 seta on the tip, which also is of the same size. Two-thirds of the middle lobe's outer rim are covered by 20 more uniform setae, which are half the size of those on the inner rim. It is about 3 times as long as the inner lobe and 4 times as long as maximum width. The outer lobe has about 70 uniform setae covering the whole rim. It is about half the size of the middle lobe and about twice as wide as long. The exopod is the largest element of appendage 5, which is surrounding the proximal and distal part. It has numerous setae around the whole rim.

Appendage 6 (maxilliped 1; Fig. 8) is differentiated into coxa, basipod with an endite, endopod,

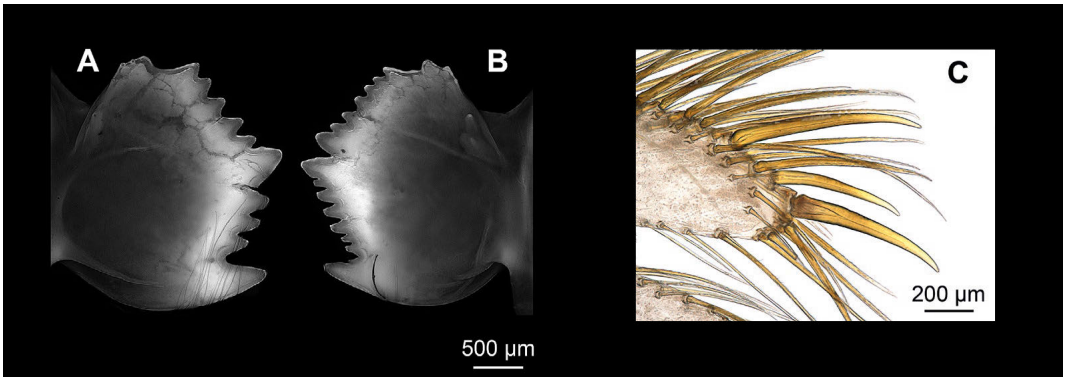

Fig. 7. Details referring to Figure 6. Fluorescence microscopic detail of the right (**A**) and left (**B**) mandibles, anterior (note the differences in armature); **C.** transmitted white-light microscopic detail of the tip of the basipodal endite of the left maxillula, anterior.

exopod and epipod. It is slightly larger than the preceding appendage. The coxa is more or less flattened triangular from anterior and posterior view. The basipod is more or less flattened tube-shaped. It is about twice as wide as the coxa and about twice as long as wide. The basipodal endite of appendage 6 is paddle-shaped and about as long as the width of the basipod. The endopod of appendage 6 consists of 3 elements with numerous setae: Endopod element 1 is more or less tube-shaped and about 5 times as long as wide. Endopod element 2 is more or less tube-shaped, slightly smaller but slightly wider than the first element and about 3 times as long as wide. Endopod element 3 is paddle-shaped, slightly bigger than the second element and about 4 times as long as maximum width. The exopod has a bilobed tip and is covered with numerous setae. It is about one third longer than and 4–5 times as wide as the endopod. The epipod is paddle-shaped, with numerous setae and about as long as the exopod.

Appendage 7 (maxilliped 2; Fig. 8) is differentiated into coxa, basipod and endopod. It is about half the size of the preceding appendage. On the inner lateral side of every element numerous setae can be seen, plus about 15 setae on the outer lateral side of the coxa. The coxa is tube-shaped with a slightly endite-like protrusion with about 15 uniform setae. It is about twice as long as maximum width. The basipod is triangular from anterior and posterior view and about as long as maximum length of coxa. The endopod of appendage 7 consists of 5 elements: Endopod element 1 (ischium) is more or less tube-shaped and about as wide as long. Endopod element 2 (merus) is more or less oval-shaped, about 3 times as long as the preceding element and about 1.3 times as long as maximum width. Endopod element 3 (carpus) is more or less kidney-shaped and about half the size of the preceding element. It is about twice as long as maximum width. Endopod element 4 (propodus) has 2 setae-like spines. It is more or less cone-shaped with a flattened tip, about two-thirds of the size of the preceding element and about twice as long as maximum width. Endopod element 5 (dactylus) is formed as a spine. It is about half the size of the preceding element, without any setae and about 3 times as long as maximum width.

Appendage 8 (maxilliped 3; Fig. 8) is differentiated into coxa, basipod and endopod with basipod and endopod not yet separated. It is about one third longer than the preceding appendage, with numerous setae on the inner lateral side and a few on the outer lateral side of every element. The coxa is more or less tube-shaped with a slightly endite-like protrusion with about 30 setae. It is about as long as maximum width. The basipod is not yet separated from the endopod but a groove is indicating a possible future joint. It is more or less triangular from anterior and posterior view. It is about half the size of the coxa at maximum length. The endopod of appendage 8 consists of 5 elements: Endopod element 1 (ischium) is more or less tube-shaped and about 3 times as long as maximum width. Endopod element 2 (merus) is more or less tube-shaped and about half the size of the preceding element. It is about twice as long as wide. Endopod element 3 (carpus) is more or less tube-shaped, about half the size of the preceding element and about twice as long as wide. Endopod element 4 (propodus) is more or less tube-shaped. It is about as long as the preceding element and about twice as long as wide. Endopod element 5 (dactylus) is more or less cone-shaped with a round tip. It is about twice as long as maximum width.

Appendage 9 (thoracopod 4; Fig. 9) is differen-

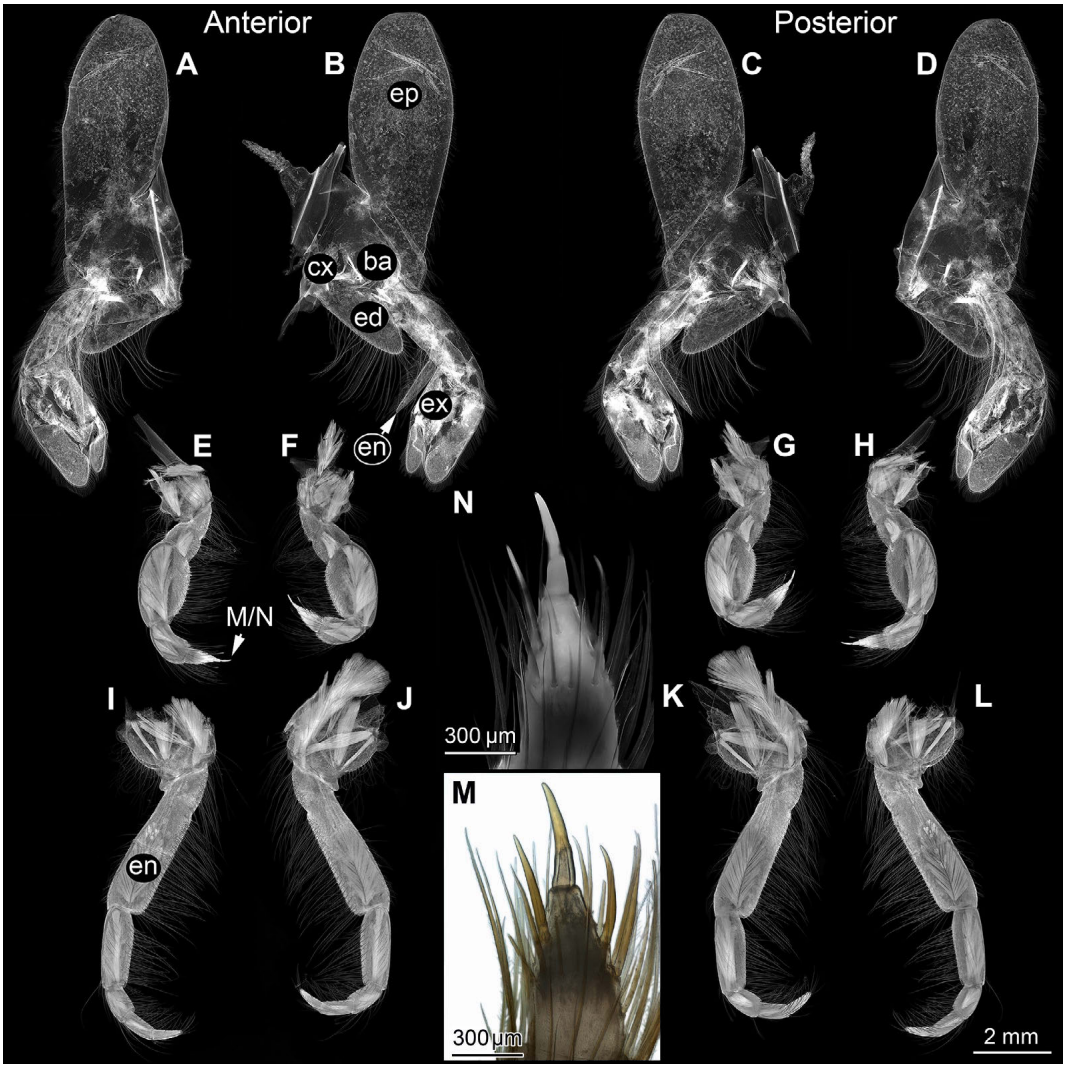

Fig. 8. Overview of mouthparts continued. **A.** Right maxilliped 1, anterior; **B.** left maxilliped 1, anterior; **C.** left maxilliped 1, posterior; **D.** right maxilliped 1, posterior; **E.** right maxilliped 2, anterior; **F.** left maxilliped 2, anterior; **G.** left maxilliped 2, posterior; **H.** right maxilliped 2, posterior; **I.** right maxilliped 3, anterior; **J.** left maxilliped 3, anterior; **K.** left maxilliped 3, posterior; **L.** right maxilliped 3, posterior; **M.** transmitted white-light microscopic detail of the maxilliped 2; **N.** fluorescence microscopic detail of the maxilliped 2. Abbreviations: **ba**, basipod; **cx**, coxa; **ed**, endite; **en**, endopod; **ep**, epipod; **ex**, exopod.

tiated into coxa, basipod and endopod. It is about 4 times as long as the preceding appendage. It has just 1 main axis consisting of 7 visible elements. The fixed finger of propodus and dactylus are forming a chela. The coxa is more or less tube-shaped, about twice as long as wide and with 5 big spines at the distal part, directed distally. The basipod is more or less tube-shaped, about half the size of the coxa and about twice as long as wide. The endopod of appendage 9 consists of 5 elements: Endopod element 1 (ischium) is more or less tube-shaped, curved and about 5 times as long as maximum width. Endopod element 2 (merus) is more or less tube-shaped, curved and about twice as long as the preceding element. It is about 6 times as long as maximum width, with about 10 small spines at the inner rim and 4 bigger spines at the outer rim of the element. Endopod element 3 (carpus) is more or less tube-shaped. It

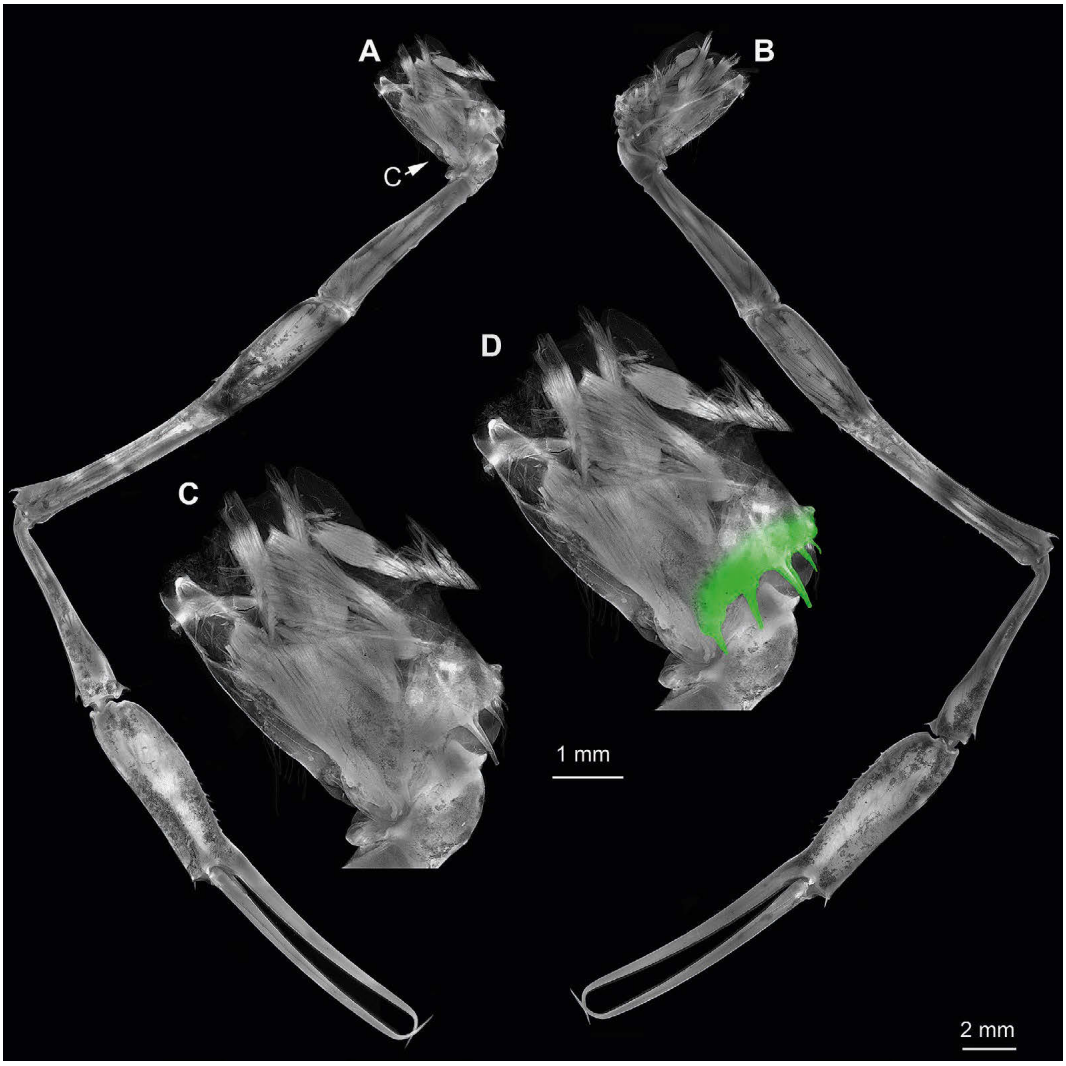

Fig. 9. Right thoracopods 4, overview. **A.** Posterior; **B.** anterior; **C.** detailed view of the coxa, posterior; **D.** detailed view of the coxa, posterior, with colour marked spines.

is about half the size of the preceding element and about 5 times as long as maximum width. It has 2 spines at the distal end of the element. Endopod element 4 (propodus) is more or less club-shaped and about twice as long as the preceding element. It has about 10 small spines at the inner rim of the bigger, proximal part of the element and one spine at the joint to the next element. The joint to the next distal element lies in the middle of the propodus (in proximal-distal axis), next to the base of the fixed finger. The fixed finger is formed as a spine with a bent tip. It is about 6 times as long as maximum width. Endopod element 5 (dactylus) is about half the size of the preceding element. It is also formed as a spine with a bent tip and it is movable against the fixed finger of the propodus. It is about 10 times as long as wide.

Appendage 10 (thoracopod 5; Fig. 10) is differentiated into coxa, basipod and endopod with basipod and endopod not yet separated. It has only 1 main axis consisting of 7 visible elements. The basipod and endopod are probably not separated by a joint, yet, but a groove is indicating a possible future joint. The fixed finger of propodus and dactylus are forming a chela. It is more or less about half the size of the preceding appendage and has numerous

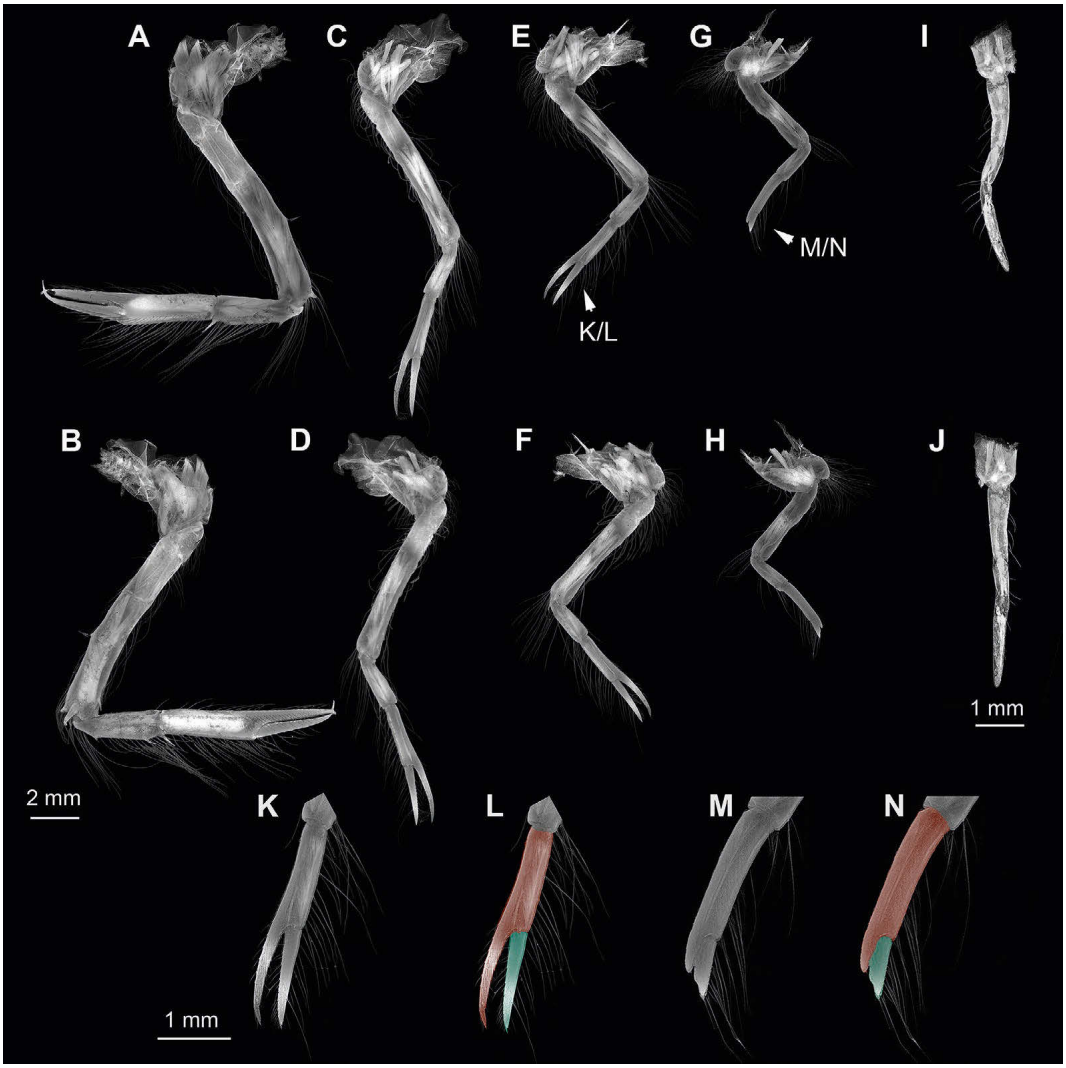

Fig. 10. Right thoracopods 5–8 (**A–H**) and left pleopod 1 (**I–J**). **A.** Thoracopod 5, anterior; **B.** thoracopod 5, posterior; **C.** thoracopod 6, anterior; **D.** thoracopod 6, posterior; **E.** thoracopod 7, anterior; **F.** thoracopod 7, posterior; **G.** thoracopod 8, anterior; **H.** thoracopod 8, posterior; **I.** pleopod 1, anterior; **J.** pleopod 1, posterior; **K.** chela of thoracopod 7, anterior; **L.** chela of thoracopod 7, anterior, with colour marked elements; **M.** chela of thoracopod 8, anterior; **N.** chela of thoracopod 8, anterior, with colour marked elements. Propodus (red), dactylus (cyan).

setae on every element. The coxa is more or less tube-shaped with an endite-like protrusion with about 5 setae. It is about twice as long as wide. The basipod is more or less triangular from anterior and posterior view and about half the size of the coxa at maximum length. The endopod of appendage 10 is not separated from the basipod yet. It consists of 5 elements whereby ischium and merus are probably not separated yet, but possible future joints between these elements are visible. Endopod element 1–2 is probably corresponding to ischium and merus, which are not separated yet. It is more or less tube shaped, curved and with 1 spine on the outer rim at about two-thirds of the element and 1 spine at the distal end with 2 setae at the tip. Endopod element 3 (carpus) is more or less tube-shaped and about half the size of the preceding element. It is about 3 times as long as wide, with 1 smaller spine at the proximal end and 1 bigger spine at the outer rim of the distal end of the element. Endopod element 4 (propodus)

is more or less club-shaped and about twice as long as the preceding element. The joint to the next distal element lies in the middle of the propodus (in proximal-distal axis), next to the base of the fixed finger. The fixed finger is formed as a spine with a bent tip. It is about 6 times as long as maximum width. Endopod element 5 (dactylus) is about half the size of the preceding element. It is also formed as a spine with a bent tip and movable against the fixed finger of propodus. It is about 5 times as long as wide.

Appendage 11 (thoracopod 6; Fig. 10) is differentiated into coxa, basipod and endopod, with basipod and endopod not yet separated. It has only 1 main axis consisting of 6 visible elements. Basipod and endopod are probably not separated by a joint yet, but a groove is indicating a possible future joint. The fixed finger of propodus and dactylus are forming a chela. It is about two-thirds of the size of the preceding appendage. It has numerous setae on every element. The coxa is more or less tube-shaped with a slightly endite-like protrusion with about 10 setae. It is about as long as maximum width. The basipod is more or less triangular from anterior and posterior view. It is about half the size of the coxa at maximum length. The endopod of appendage 11 is not separated from the basipod yet. It consists of 4 visible elements whereby ischium and merus are not separated yet, and no possible future joint is visible. Endopod element 1–2 is probably corresponding to ischium and merus, which are not separated yet. It is more or less tube-shaped, curved and about 5 times as long as wide. Endopod element 3 (carpus) is more or less tube-shaped. It is about half the size of the preceding element and about 3 times as long as wide. Endopod element 4 (propodus) is more or less club-shaped. The joint to the next distal element lies in the middle of the propodus (in proximal-distal axis), next to the base of the fixed finger. It is about twice as long as the preceding element and about 6 times as long as maximum width. Endopod element 5 (dactylus) is about half the size of the preceding element. It is formed as a spine and movable against the fixed finger of propodus. It is about 6 times as long as wide.

Appendage 12 (thoracopod 7; Fig. 10) is differentiated into coxa, basipod and endopod, with basipod and endopod not yet separated. It has only 1 main axis consisting of 6 visible elements. Basipod and endopod are probably not separated by a joint yet, but a groove is indicating a possible future joint. The fixed finger of propodus and dactylus are forming a chela. It is about two-thirds of the size of preceding appendage. It has numerous setae on every element. The coxa is more or less tube-shaped and with an endite. It is about as wide as long. The endite is paddle-shaped and with numerous setae. It is about as long as maximum width. The basipod is more or less triangular from anterior and posterior view. It is about as long as the coxa at maximum length. The endopod of appendage 12 is not separated from the basipod yet. It consists of 4 visible elements. Ischium and merus are probably not separated yet, and no possible future joint is visible. Endopod element 1–2 is probably corresponding to ischium and merus, which are not separated yet. It is more or less tube-shaped and about 4 times as long as wide. Endopod element 3 (carpus) is more or less tube-shaped. It is about half the size of the preceding element and about twice as long as wide. Endopod element 4 (propodus) is more or less club-shaped, about twice as long as the preceding element and about 6 times as long as maximum width. The joint to the next distal element lies in the middle of the propodus (in proximal-distal axis), next to the base of the fixed finger. Endopod element 5 (dactylus) is about half the size of the preceding element and about 6 times as long as maximum width. It is formed as a spine and movable against the fixed finger of propodus.

Appendage 13 (thoracopod 8; Fig. 10) is differentiated into coxa, probably basipod (not yet visible) and endopod. It has only 1 main axis consisting of 5 visible elements. Probably basipod and endopod are not separated yet, and no possible future joint is visible. The fixed finger of propodus and dactylus are forming a beginning chela, which is presumably not yet fully developed because either propodus and dactylus are reduced or they are not fully developed yet. It is about two-thirds of the size of the preceding appendage. The coxa is more or less tube-shaped and with an endite. It has 2 spines on the distal part of the outer lateral rim. It is about as long as wide. The endite is paddle-shaped and with numerous setae. It is about as long as maximum width. The endopod of appendage 13 is probably not separated from the basipod yet. It consists of 4 visible elements. Ischium and merus are probably not separated yet, and no possible future joint is visible. Endopod element 1–2 is probably corresponding to ischium and merus, which are not separated yet. It is more or less tube-shaped and with about 5 setae at the joint to the next element. It is about 4 times as long as wide. Endopod element 3 (carpus) is more or less tube-shaped. It is about half the size of the preceding element and about 3 times as long as wide. It has about 5 setae. Endopod element 4 (propodus) is slightly longer than the preceding element. The joint to the next distal element lies in about three-fourth of the propodus (in proximal-distal axis), next to the base of the fixed finger. The fixed finger is presumably not yet fully developed. It has about 10 setae; endopod element 5 (dactylus) is more or

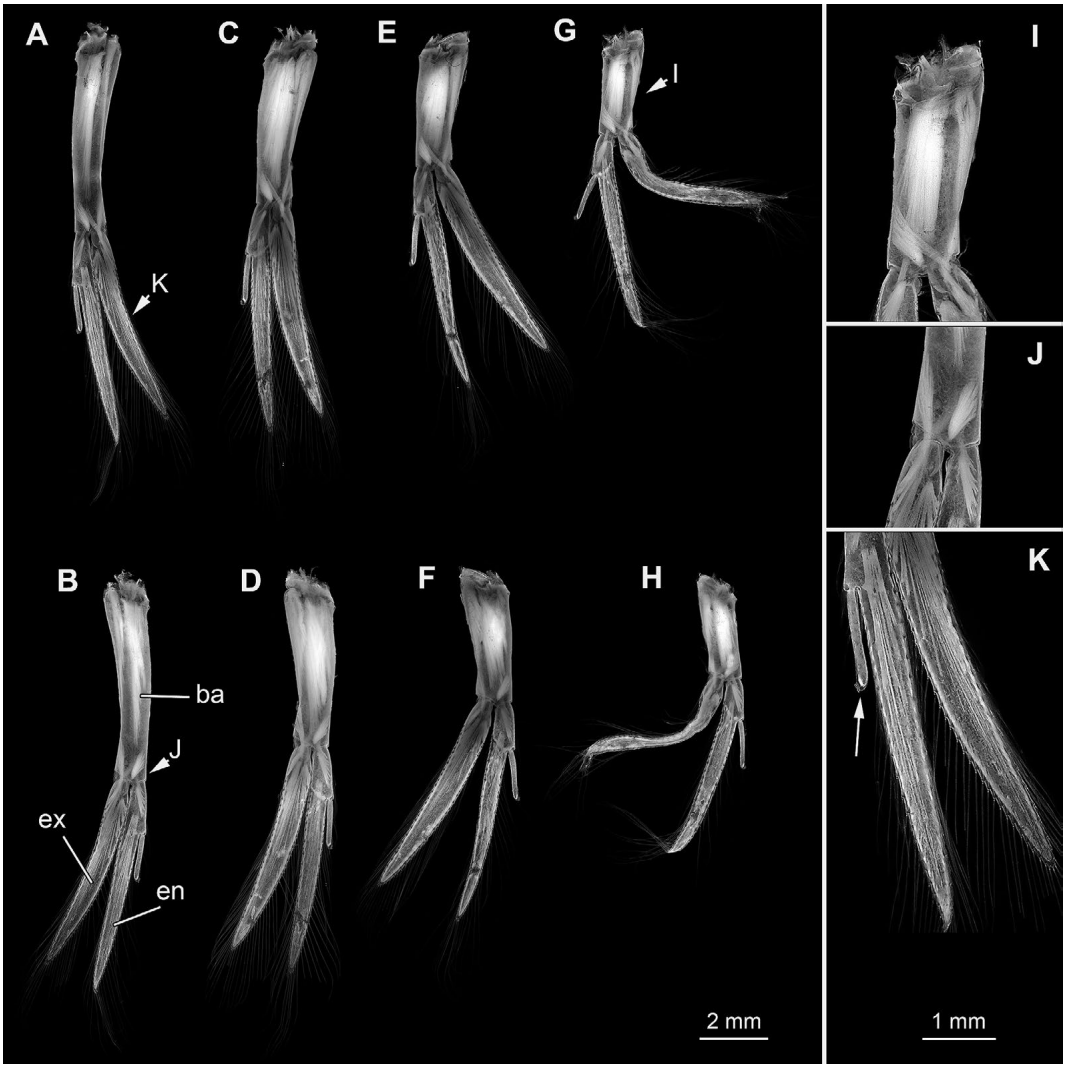

Fig. 11. Left pleopods 2-5. **A.** Pleopod 2, anterior; **B.** pleopod 2, posterior; **C.** pleopod 3, anterior; **D.** pleopod 3, posterior; **E.** pleopod 4, anterior; **F.** pleopod 4, posterior; **G.** pleopod 5, anterior; **H.** pleopod 5, posterior; **I.** detail of the basipod with muscles; **J.** detail of muscles; **K.** detail of the exo- and endopod with process (arrow). Abbreviations: **ba**, basipod; **en**, endopod; **ex**, exopod.

less tube-shaped, about one third of the size of the preceding element and about 3 times as long as wide. Presumably it is not yet fully developed but it seems to be movable against the fixed finger of propodus. It has about 10 setae.

Appendage 14 (pleopod 1; Fig. 10) is differentiated into a proximal and a distal part. Probably the proximal part is representing the basipod and the distal part is representing the endopod as in the following appendages. It has about 15 uniform setae on the outer rim of the endopod. It is about one third of the size of the preceding appendage and about 10 times as long as wide. The proximal part is tube-shaped and about as long as wide. The distal part is consisting of 1 thin paddle-shaped element. Probably it is not fully developed yet.

Appendage 15 (pleopod 2; Fig. 11) is differentiated into basipod, endopod and exopod. It has numerous and uniform setae around the whole rim of the endopod and exopod. It is about twice as long as the preceding appendage. The basipod is elongate tube-shaped and about 4 times as long as wide. The

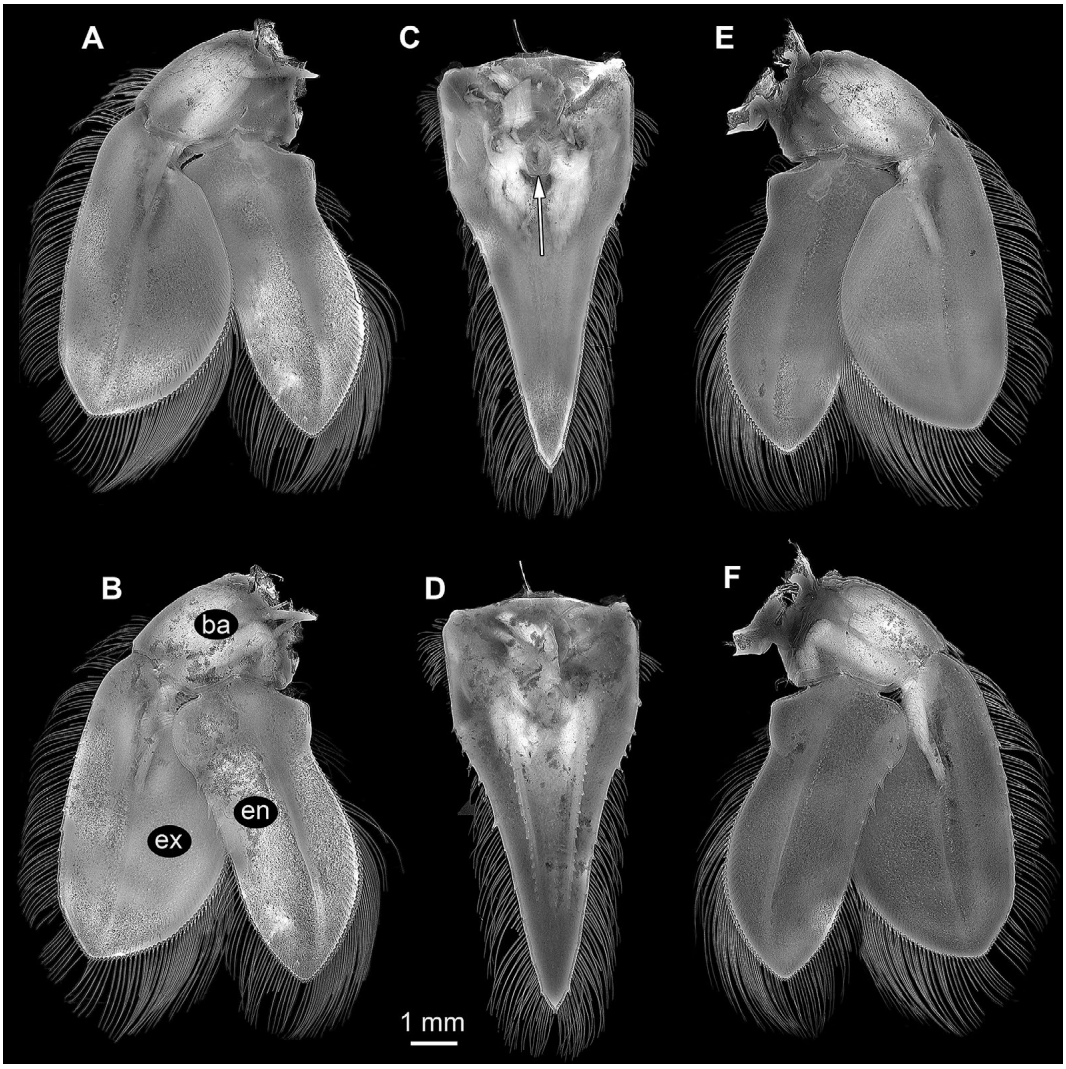

Fig. 12. Uropods and telson. **A.** Right uropod, anterior; **B.** right uropod, posterior (flipped horizontally); **C.** telson, ventral with after (arrow); **D.** telson, dorsal (flipped horizontally); **E.** left uropod, anterior; **F.** left uropod, posterior (flipped horizontally). Abbreviations: **ba**, basipod; **en**, endopod; **ex**, exopod.

endopod of appendage 15 is paddle-shaped with a tube-shaped process on the inner lateral edge (appendix interna). It is about 8 times as long as wide. The appendix interna is about one fourth of the endopod length. The exopod of appendage 15 is paddle-shaped and about 8 times as long as wide.

Appendage 16 (pleopod 3; Fig. 11) is differentiated into basipod, endopod and exopod. It has numerous and uniform setae around the whole rim of the endopod and exopod. It is about as long as the preceding appendage. The basipod is elongated tube-shaped, slightly shorter than the basipod of the preceding appendage and about 3 times as long as wide. The endopod of appendage 16 is paddle-shaped with a tube-shaped process on the inner lateral edge (appendix interna). It is as long as the endopod of the preceding appendage and about 8 times as long as wide. The appendix interna is about one fourth of the endopod length. The exopod of appendage 16 is paddle-shaped, as long as the exopod of the preceding appendage and about 8 times as long as wide.

Appendage 17 (pleopod 4; Fig. 11) is differentiated into basipod, endopod and exopod. It has numer-

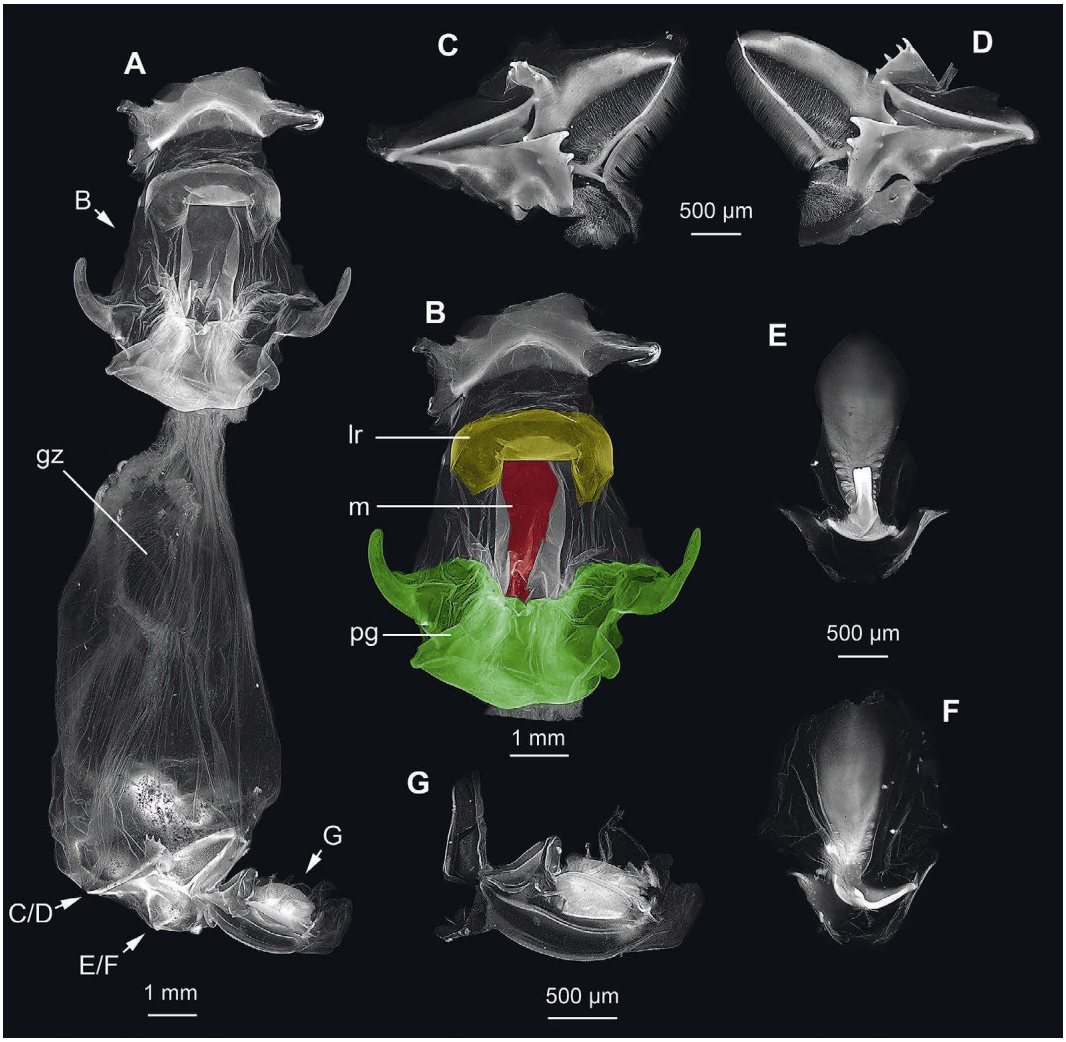

Fig. 13. **A.** Labrum (**lr**), mouth (**m**), paragnaths (**pg**) and gizzard (**gz**) overview; **B.** colour marked detailed view of labrum (yellow), mouth (red) and paragnaths (green); **C–D.** lateral gizzard teeth; **E.** median gizzard tooth; **F.** median gizzard tooth, lateral view; **G.** reusen-apparatus.

ous and uniform setae around the whole rim of the endopod and exopod. It is slightly smaller than the preceding appendage. The basipod is tube-shaped and slightly shorter than the basipod of the preceding appendage. It is about twice as long as wide. The endopod of appendage 17 is paddle-shaped with a tube-shaped process on the inner lateral edge (appendix interna). It is as long as the endopod of the preceding appendage and about 8 times as long as wide. The appendix interna is about one fourth of the endopod length. The exopod of appendage 17 is paddle-shaped, as long as the exopod of the preceding appendage and about 8 times as long as wide.

Appendage 18 (pleopod 5; Fig. 11) is differentiated into basipod, endopod and exopod. It has numerous and uniform setae around the whole rim of the endopod and exopod. It is slightly smaller than the preceding appendage. The basipod is tube-shaped and slightly shorter than the basipod of the preceding appendage. It is about twice as long as wide. The endopod of appendage 18 is paddle-shaped with a tube-shaped process on the inner lateral edge (appendix interna). It is slightly shorter than the endopod of the preceding appendage and about 7 times as long as wide. The appendix interna is about one fourth of endopod length. The exopod

of appendage 18 is paddle-shaped, slightly shorter than the exopod of the preceding appendage and about 7 times as long as wide.

Appendage 19 (uropod; Fig. 12) is differentiated into basipod, endopod and exopod. It is about as long as the preceding appendage. The basipod is more or less heart-shaped. It has about 20 setae. It is about as long as maximum width. The endopod is paddle-shaped with a strongly convex inner edge with 3 spines and with about 130 setae around the whole rim. The exopod is paddle-shaped with a slightly concave outer edge and with about 140 setae around the whole rim.

The gizzard (Fig. 13) is sack-like and it emanates from the mouth opening. It has 2 lateral and 1 median gizzard tooth in it at the distal end. The distal end appears to pass into a reusen-apparatus.

The lateral gizzard teeth (Fig. 13) are triangular. The longest side is oriented laterally, the shortest side is oriented medio-anteriorly. The medio-anterior edge is equipped with numerous setae. The central surface of the triangle is elevated to form an anteriorly oriented edge with at least 4 teeth. The teeth are decreasing in size from lateral to median. The lateral edge is protruded into an enditic structure with 5 teeth.

The median gizzard tooth (Fig. 13) is hook-shaped. Its basal plate has about 7 teeth on each side, which appear to be grinding teeth, while the hook appears to be one big tooth. It is about half the size of the lateral gizzard teeth.

The reusen-apparatus is more or less u-shaped and surrounding a starfruit-shaped structure. It is about as big as the median gizzard tooth.

Discussion

Method evaluation

Autofluorescence imaging has been demonstrated as a successful method for documenting crustaceans and so has been applied on other crustacean larvae before (HaugC et al. 2012, Kutschera et al. 2012, Rötzer & HaugJT 2015); hence, it was used for examining the eryoneicus larva in this study. This method allows documentation of the material directly in alcohol without drying artefacts (HaugJT et al. 2011a, HaugC & HaugJT 2014) that are often coupled to documentation with scanning electron microscopy (SEM). Furthermore, it is possible to examine historical museum material without any chemical staining (Kutschera et al. 2012). And, lastly, even internal structures become visible such as muscle details (HaugJT et al. 2014, see also Fig. 11).

Additionally, stereo imaging under polarised light was applied, also in alcohol, that made it possible to document the material without disturbing reflections (HaugC & HaugJT 2014). Moreover, this method provides a good 3D impression of the structures, for example, the dimension of the highly inflated shield that is lost in normal 2D photographs. If SEM would be applied for documentation it would not be possible to dissect the larva after drying. But as stereo imaging is not destroying the material, it could still be dissected for documentation with autofluorescence imaging. This procedure also keeps the material available for further studies with other methods.

Comparison with previous work on polychelidan larvae

The previously examined material of eryoneicus larvae has mostly been documented with overview photographs (e. g. Tiefenbacher 1982, 1994, Boyko 2006), but usually lacking close-ups of structural details. In certain cases, relatively high-resolution overview photographs have been presented (Martin 2014a, Torres et al. 2014), but close-ups have only been documented under SEM (one counterexample by Hernández et al. 2007). Additionally, line drawings, both of an overview of the larvae (e. g. Bernard 1953, Williamson 1983, Martin 2014a) and of detailed structures such as rostrum, antennae, mouthparts and limbs (Bernard 1953, Torres et al. 2014) are available. Furthermore, also adult polychelidan lobsters have been documented with overview photographs (Boyko 2006) and more detailed photographs of shield and pleon (Galil 2000). But also overview line drawings of adult polychelid lobsters have been presented (Galil 2000, Ahyong 2009) as well as line drawings of detailed structures such as mouthparts (Galil 2000) and other limbs.

With this study, we provide the first detailed photo documentation with high-quality overview stereo images and detailed high magnification (autofluorescence) images of a dissected eryoneicus larva. This made it possible to describe very tiny details of outer structures such as thoracopods and pleopods, but also inner structures such as the gizzard.

Identification of the investigated larva

A complete determination of the species of the larva is not possible. The examined larva is labelled as *"Eryoneicus" atlanticus*, but it is still not clear if this determination is correct. Comparing the larva with the detailed line drawings of many different eryoneicus larvae by Bernard (1953) it seems to

have similarities to an *"E." atlanticus* such as the rostrum. However, the examined larva also seems to have a little epipodite on the third maxilliped, which is a striking trait for *Stereomastis* sp. (Ahyong pers. comm. 2014).

Another difficult but important issue is the identification which "adult species" the investigated larva belongs to. As mentioned above, eryoneicus larvae have commonly been described as separate species before it became clear that they are the larvae of polychelidan lobsters. Unfortunately, it was only rarely possible to determine which larva belongs to which adult (Guerao & Abelló 1996, Torres et al. 2014, discussion in Gurney 1942, Martin 2014a).

Since it is very difficult to hatch and rear deep-sea crustaceans under unnatural conditions in captivity to identify the larvae with their corresponding adults (successful attempts by Guerao & Abelló 1996), another method has to be applied. DNA barcoding could be a solution for analysing already collected specimens whereby it has to be respected that not all museum material can be adduced for that method. Recently, Torres et al. (2014) applied the first DNA analysis on polychelidan larvae; in this study, they identified *"Eryoneicus" puritanii* as a larval stage of *Polycheles typhlops* (see Tang et al. 2010 for a similar DNA barcoding study on stomatopods). A widespread analysis has to be done so that almost every yet known larval type of polychelidans can be identified with the corresponding adult. However, such a DNA analysis by itself would not be enough. Also morphological analyses have to be applied to the different ontogenetic stages of the species to be identified. In summary, although it is not possible to determine the species of the here investigated larva, this study contributes important new insights on the biology of polychelidan larva.

Developmental pattern

According to Torres et al. (2014) there are only three zoea stages in the polychelidan species investigated by them, thus there have to be several megalopa stages to reach the final size as they can reach a size of several centimeters. Usually modern reptantians have only one megalopa stage (but see discussion in HaugJT & HaugC 2013, HaugJT et al. 2013a). Based on the size, the specimen investigated here is probably a late megalopa.

Such a developmental pattern is probably a specialization to a long life in a pelagic habitat. This brings many advantages, especially in dispersal and avoiding intraspecific competition between the larval and the juvenile/adult forms (more details will be discussed below).

Development of morphological structures

In general, the appendages of the investigated larva appear to be already fully developed (although it is equivocal for the mouthparts, see ecological discussion below). However, for the thoracopods 5–8 the development might not be complete yet on this larva. They seem not to be fully developed yet, because of visible grooves that are indicating future joints between the not yet divided basipods and endopods and further between ischium and merus, where in thoracopod 5 a future joint is already visible. On the other hand, it is also possible that basipod, ischium and merus are not going to get divided by a joint, so that development of these legs will get stopped at some time. The latter would be in accordance with Scholtz & Richter (1995) who described this phenomenon as an apomorphic character of adult polychelidans.

At the first pleomere of the investigated larva, the tergo-pleura are developed into hook-like structures, which connect the pleon with the shield. Such a structure is also found in adult polychelidans, but there is only a similar structure like this known in achelates, but in no other decapod group (Scholtz & Richter 1995). Probably, these structures, together with the numerous setae covering the posterior rim of the shield, support a complete closing mechanism of the shield. Due to the hook-like structures this closed position does not need to be held by the muscles of the pleon. With this, the cavity of the shield would be totally isolated from the environment.

Functional morphology as a key to autecology

As it is difficult to investigate ecology and behaviour of deep-sea species directly, it is necessary to discuss the functional morphology based on the findings made on the examined larva. Based on functional aspects, certain conclusions are possible about autecology and behaviour (HaugC & HaugJT 2014).

1) Shield (carapace)

Modern polychelids develop from highly specialized larvae that are characterized by a strongly inflated and spiny shield. But these larvae are not the only ones which are known to have such a type of shield. Also in Stomatopoda a larval form is known that has a bulged spiny shield: the erichthus-type larva (e. g. see Gamô 1979, HaugC & HaugJT 2014, their fig. 4). Such a shield form reminds of a balloon and seems to be a successful specialization to a life in pelagic water. Also among different brachyuran larvae bulging shields with floatation spines have evolved repeatedly. Numerous types of zoea-larvae possess a

rather bulging shield with longer spines (e. g. Martin 2014b, his figs 54.3–5) but are comparably smaller. Yet also among the larger (and later) megalopa larvae forms have evolved with comparably shields, for example in Homolidae (Martin 2014b, his fig. 54.8E) or Inachidae (Martin 2014b, his fig. 54.9B–D). The shield of the eryoneicus larva has numerous setae covering the posterior and ventral edge. The narrowly adjacent setae seem to form a barrier that prevents particles to invade into the shield (see also HaugJT et al. 2011b).

2) Mouthparts

The morphology and structure of the mouthparts observed in this study can lead to several hypotheses. Bernard (1953) had examined the stomach content of a specimen of *"Eryoneicus" puritanii* and discovered that they are feeding on plankton such as cnidarians, cyanobacterias, diatoms or coccolithophores. This observation is also supported by our examination on the mouthparts. The maxilla with its big exopodite and the maxilliped 1 with its large paddle-shaped epipodite and big bilobed exopod seem to be responsible for creating a water current into the mouth opening. With maxillipeds 2 and 3 covered with numerous and relatively big setae on the inner lateral rim they seem to be applicable for "filtering" the water for larger edible particles such as plankton.

Yet, on the other hand, the mouthparts also show some traits that can lead to another hypothesis: with the maxillula having setae-like spines at the tip of the basipodal endite and maxilliped 2 having a dactylus formed as a spine, it seems that the larva's mouthparts are feasible for catching and holding bigger prey. Additionally, the mandibles have a long coxa and the joint is situated far laterally, which results in a very long lever (see HaugJT et al. 2012 and HaugJT et al. 2014 for discussion of lateral position of appendage joints). With this and a corresponding strong musculature it should be possible for the larva to accomplish a great bite force. Furthermore, the different numbers of mandible teeth and their position to each other show that they are interlocking during chewing so that masticating should be easier. These traits lead to the assumption that the larva is not just feeding on plankton by "filtration" but seems also to be an active predator. As the gizzard with its masticatory organs was detected as well, this hypothesis seems to be fairly reasonable.

This leads to three hypotheses:

1) The larva is still just a filter feeder, but the developed mandibles and (setae-like) spines on maxillula and maxilliped 2 as well as the gizzard are part of a step-wise development of the feeding apparatus of the adult.
2) The larva developed into an active predator and the filtering function of the mouthparts is becoming reduced, which could be approved by the very few musculature in the maxilla (only retained in the proximal part; Figure 6) and the obviously missing musculature in maxilliped 1 (Figure 8).
3) The larva developed both mouthparts for filtration and active predating as this is another specialization to a pelagic life in the deep sea where it is difficult to find prey and the detritus coming from shallower water is the supplement food. There are indeed examples from other crustaceans for the evolution of such a generalistic lifestyle, which may lead to a large evolutionary success (e. g. Mayer et al. 2008 for an amphipod) Also the well developed and long thoracopod 4 and its chela may be evidence for the hypotheses that the larva is (also) an active predator.

3) Adaptation to long life in pelagic water

As mentioned above, polychelidans seem to have more than just one megalopa stage during their larval development. This is probably an adaptation to a long life in pelagic water. A benefit of such a developmental pattern is likely a decrease of competition between larvae and conspecific juveniles and adults. When different life stages exploit the same resources they are indirect competitors in the form of exploitation competition.

As the larvae inhabit a pelagic habitat they are spatially separated from the juveniles/adults that are inhabitants of the benthos.

In this way, the larval development is not further interfering with the juveniles/adults, i. e. they are not competing of the same resources. The larvae are only exposed to competition by other pelagic exploitation competitors or direct competitors.

Furthermore, when the larvae are finally shifting to the benthos they might already have moved into new areas where their juvenile/adult forms are less represented, whereby a decrease of exploitation competition is given again (see also next point for this aspect).

4) Dispersal

Many benthic organisms develop through a pelagic larval phase. This improves the organisms' ability of dispersal as the mobility of pelagic larvae is relatively easy due to water currents, while benthic forms would have to overcome many obstacles to reach new areas for living.

As the polychelidans have developed larval forms that are highly specialized to a long life in

pelagic water, a requirement for a very wide dispersal is given: The longer the pelagic phase lasts, the longer the distances are that can be overcome by the larvae.

Such a wide dispersal has many advantages such as avoiding exploitation competition (as mentioned above). Furthermore, the cosmopolitan occurrence of many deep-sea species hints to a successful dispersal strategy. Nevertheless, the question remains how representatives of one species can find each other.

5) Settling

As there is nothing known about the settling behaviour and possible triggers in polychelidan larvae, one can only assume which mechanisms or conditions initiate the shift to benthic life. It could be possible that the larvae are settling to the benthos in groups as this is probably accompanied with moulting to the benthic juvenile phase. A high density of individuals during moulting, i. e. when the individuals are vulnerable to predators, is decreasing predator pressure (see discussion in HaugJT et al. 2013b). Hence, it is possible that the larvae either occur in swarms/schools during their pelagic life, which also would have the advantage of decreasing predator pressure, or they have to find each other for settling. A possible explanation for the latter case could be communication mechanisms by taking advantage of hormones such as pheromones (HaugJT et al. 2013b). Furthermore, such mechanisms for finding each other will probably be important during the juvenile phase, also for example for finding together in aggregations for moulting in groups of a high number of individuals (e. g. HaugJT et al. 2013b and references therein). Finally, living together in groups in the deep sea would reduce the time to find a mating partner in the adults.

Outlook

Examination of the mouthparts leads to three hypotheses that only can be corroborated by an extensive research on feeding behaviour of polychelidan larvae as there is almost nothing known about their ecology and behaviour. Furthermore, it is important to identify larvae with their corresponding adults. First attempts have been made, but this is still not enough. To get a more exact knowledge of the polychelidans, more analyses have to be performed, especially with more detailed examinations and presentations of the results.

Acknowledgements

Many thanks to all the persons and institutions without whose help this study would not have been possible. For providing access to the technical equipment we would like to thank Prof. Dr. J. Matthias Starck. To the Muséum National d'Histoire Naturelle in Paris many thanks for providing the examined material. Furthermore we would like to thank all people spending their time for programming free or extremely low cost software such as Combine ZM/ZP and Microsoft Image Composite Editor. CH is kindly funded by the Bavarian Equal Opportunities Sponsorship of the LMU Munich. This project is part of JTH's project "Palaeo-Evo-Devo of Malacostraca" kindly funded by the German Research Foundation (DFG) under Ha 6300/3-1.

References

Ahyong, S. T. 2009. The Polychelidan lobsters: phylogeny and systematic (Polychelida: Polychelidae). Pp. 369–396 in: Martin, J. W., Crandall, K. A. & Felder, D. L. (eds). Decapod crustacean phylogenetics. Crustacean Issues, vol. 18. New York (CRC Press).

– – 2012. Polychelid lobsters (Decapoda: Polychelida: Polychelidae) collected by the CIDARIS expeditions off Central Queensland, with a summary of Australian and New Zealand distributions. Memoirs of the Queensland Museum, Nature 56 (1): 1–8.

Bernard, F. 1953. Decapoda Eryonidae (*Eryoneicus* et *Willemoesia*). Dana-Report 37: 1–93.

Boyko, C. B. 2006. New and historical records of polychelid lobsters (Crustacea: Decapoda: Polychelidae) from the Yale Peabody Museum Collections. Bulletin of the Peabody Museum of Natural History 47 (1–2): 37–46.

Galil, B. S. 2000. Crustacea Decapoda: review of the genera and species of the family Polychelidae Wood-Mason, 1874. Pp. 285–387 in: Crosnier, A. (ed.). Résultats des campagnes MUSORSTOM, vol. 21. Mémoires du Muséum National d'Histoire Naturelle (France) 184.

Gamô, S. 1979. Notes on a giant stomatopod larva taken south-east of Mindanao, Philippines (Crustacea). Science Reports Yokohama National University, Sect. 2 Biological and Geological Sciences 26: 11–17.

Guerao, G. & Abelló, P. 1996. Description of the first larval stage of *Polycheles typhlops* (Decapoda: Eryonidea: Polychelidae). Journal of Natural History 30 (8): 1179–1184.

Gurney, R. 1942. Larvae of decapod Crustacea. London (The Ray Society).

Haug, C. & Haug, J. T. 2014. Defensive enrolment in mantis shrimp larvae (Malacostraca: Stomatopoda). Contributions to Zoology 83 (3): 185–194.

– – , Mayer, G., Kutschera, V., Waloszek, D., Maas, A. & Haug, J. T. 2011. Imaging and documenting gammarideans. International Journal of Zoology: article ID 380829. doi:10.1155/2011/380829

– – , Sallam, W. S., Maas, A., Waloszek, D., Kutschera, V. & Haug, J. T. 2012. Tagmatization in Stomatopoda – reconsidering functional units of modern-day mantis shrimps (Verunipeltata, Hoplocarida) and implications for the interpretation of fossils. Frontiers in Zoology 9: art. 31.

– – , Shannon, K. R., Nyborg, T. & Vega, F. J. 2013. Isolated mantis shrimp dactyli from Pliocene of North Carolina and their bearing on the history of Stomatopoda. Boletín de la Sociedad Geológica Mexicana 65 (2): 273–284.

Haug, J. T. & Haug, C. 2013. An unusual fossil larva, the ontogeny of achelatan lobsters, and the evolution of metamorphosis. Bulletin of Geosciences 88 (1): 195–206.

– – , Haug, C. & Ehrlich, M. 2008. First fossil stomatopod larva (Arthropoda: Crustacea) and a new way of documenting Solnhofen fossils (Upper Jurassic, Southern Germany). Palaeodiversity 1: 103–109.

– – , Haug, C., Kutschera, V., Mayer, G., Maas, A., Liebau, S., Castellani, C., Wolfram, U., Clarkson, E. N. K. & Waloszek, D. 2011a. Autofluorescence imaging, an excellent tool for comparative morphology. Journal of Microscopy 244: 259–272.

– – , Olesen, J., Maas, A. & Waloszek, D. 2011b. External morphology and post-embryonic development of *Derocheilocaris remanei* (Crustacea: Mystacocarida) revisited, with a comparison to the Cambrian taxon *Skara*. Journal of Crustacean Biology 31: 668–692.

– – , Briggs, D. E. G. & Haug, C. 2012. Morphology and function in the Cambrian Burgess Shale megacheiran arthropod *Leanchoilia superlata* and the application of a descriptive matrix. BMC Evolutionary Biology 12: art. 162.

– – , Audo, D., Charbonnier, S. & Haug, C. 2013a. Diversity of developmental patterns in achelate lobsters – today and in the Mesozoic. Development Genes and Evolution 223: 363–373. doi:10.1007/s00427-013-0452-x

– – , Caron, J.-B. & Haug, C. 2013b. Demecology in the Cambrian: synchronized molting in arthropods from the Burgess Shale. BMC Biology 11: art. 64.

– – , Audo, D., Haug, C., Saad, P. A., Petit, G. & Charbonnier, S. 2015. Unique occurrence of polychelidan lobster larvae in the fossil record and its evolutionary implications. Gondwana Research 28 (2): 869–874. doi:10.1016/j.gr.2014.05.004

– – , Haug, C., Schweigert, G. & Sombke, A. 2014. The evolution of centipede venom claws – open questions and possible answers. Arthropod Structure & Development 43: 5–16.

Hernández, F. A., De Vera, A. & León, M. E. 2007. *Eryoneicus puritanii* Lo Bianco, 1903 captured in waters of Cape Verde (Reptantia: Polychelidae: Decapoda). Vieraea 35: 51–56.

Johnson, M. W. 1951. A giant phyllosoma larva of a loricate crustacean from the tropical Pacific. Transactions of the American Microscopical Society 70: 274–278. doi:10.2307/3223060

Kerp, H. & Bomfleur, B. 2011. Photography of plant fossils – new techniques, old tricks. Review of Palaeobotany and Palynology 166: 117–151.

Kutschera, V., Maas, A., Waloszek, D., Haug, C. & Haug, J. T. 2012. Re-study of larval stages of *Amphionides reynaudii* (Malacostraca: Eucarida) with modern imaging techniques. Journal of Crustacean Biology 32: 916–930. doi:10.1163/1937240X-00002092

Martin, J. W. 2014a. Polychelida. Pp. 279–282 in: Martin, J. W., Olesen, J. & Høeg, J. T. (eds). Atlas of crustacean larvae. Baltimore (Johns Hopkins University Press).

– – 2014b. Brachyura. Pp. 295–310 in: Martin, J. W., Olesen, J. & Høeg, J. T. (eds). Atlas of crustacean larvae. Baltimore (Johns Hopkins University Press).

Mayer, G., Maas, A. & Waloszek, D. 2008. Mouthparts of the Ponto-Caspian invader *Dikerogammarus villosus* Sowinsky, 1894 (Gammaridae). Journal of Crustacean Biology 28 (1): 1–15.

Rötzer, M. A. I. N. & Haug, J. T. 2015. Larval development of the European lobster and how small heterochronic shifts lead to a more pronounced metamorphosis. International Journal of Zoology, art. 345172.

Scholtz, G. & Richter, S. 1995. Phylogenetic systematics of the reptantian Decapoda (Crustacea, Malacostraca). Zoological Journal of the Linnean Society 113: 289–328.

Tang, R. W. K., Yau, C. & Ng, W.-C. 2010. Identification of stomatopod larvae (Crustacea:Stomatopoda) from Hong Kong waters using DNA barcodes. Molecular Ecology Resources 10: 439–448.

Torres, A. P., Palero, F., Dos Santos, A., Abelló, P., Blanco, E., Boné, A. & Guerao, G. 2014. Larval stages of the deep-sea lobster *Polycheles typhlops* (Decapoda, Polychelida) identified by DNA analysis: morphology, systematic, distribution and ecology. Helgoland Marine Research 68 (3): 379–397. doi:10.1007/s10152-014-0397-0

Tiefenbacher, L. 1982. *Eryoneicus* aus Fängen von F.S. "Meteor" im mittleren äquatorialen Atlantik (Decapoda, Reptantia, Polychelidae). Spixiana 5 (1): 47–50.

– – 1994. Decapod Crustacea of western Antarctic waters collected by the R.V. "John Biscoe", cruise 11. Spixiana 17 (1): 13–19.

Williamson, D. I. 1983. Crustacea Decapoda: larvae. VIII. Nephropidea, Palinuridea, and Eryonidea. Fiches d 'Identification du Zooplancton No. 167/168. 8 pp., Copenhagen (ICES).